Pranav Mohan

February 18, 2018

Chapter 5
Fatigue Tests/Models, Failure Criteria and Fatigue Failure Mechanisms

Project 1
Fatigue Analysis of Wheel Lug Stud/Wheel lug bolt

Vehicle:
Toyota RAV4 XLE 2015

Wheel Lug Stud

AME 3353
Design of Mechanical Components
Professor H. L. Stalford

5.1 Fatigue Failure Mechanisms

In this section, we are going to explore the various fatigue failure mechanisms a ductile material like steel, which is what the lug stud is made of, can go through. Fatigue is defined as "the weakening of a material caused by repeatedly applied loads[1]." As we have seen in the previous sections, when the car goes through a circular turn, external stresses act on the lug stud. Since a car turns atleast a 1,000,000 times in its lifetime, we are interested in exploring numerous theories that describe the behaviour of a material when it goes through these fatigue cycles. The material lug stud is made out of is steel, which is a ductile material in comparison to iron, which is brittle.

One of these failure theories is the maximum distortion energy theory. It is believed that this theory was introduced by James Clerk Maxwell in the 19th century and later again by von Mises et al in the 20th century. This was the first time, the scientists were thinking of micromechanics of the materials, as previously only large scaled models were tested in mechanics of materials. They had an idea that when a material is placed in tension in the axial direction, some change in the shape and volume takes place, and this happens due to a release of distortion energy stored in the atoms. This was because they found that a material could withstand a tremendous amount of compression without failure[2]. Therefore, they concluded that a material has a limited capacity of distortion energy in it. This is shown in the figure 5.1-1 in the blue elliptical shape. This figure is modified with the courtesy of Fundamentals of Machine Component Design by Robert C. Juvinall and Kurt M. Marshek[2]. The equivalent stress can be calculated by equation 5.1-2 below where σ_1 and σ_2 are principal stresses. This equivalent stress (σ_e) value is compared to the yield stress value.

$$\sigma_e = (\sigma_1^2 + \sigma_2^2 - \sigma_1\sigma_2)^{0.5} \tag{5.1-1}$$

The equation above is derived from von Mises equation (equation 5.1-2). This equivalent stress value is supposed to produce the same value of stress as the distortion energy would produce. Equation 5.1-2 is the case for when it is a biaxial loading and, therefore, σ_3 is 0.

$$\sigma_e = \frac{\sqrt{2}}{2}[(\sigma_2 - \sigma_1)^2 + (\sigma_3 - \sigma_1)^2 + (\sigma_3 - \sigma_2)^2]^{0.5} \tag{5.1-2}$$

In a similar fashion, maximum shear stress theory also exists. This is supposed to be the oldest failure theory. However, in this case we take into account the shear stress. The theory predicts that when the maximum shear stress exceeds the maximum yield shear stress, the material tends to fatigue and fail. The other models are dependent on the principle stresses, however, this particular model takes into account the shear stress into account. This is shown by the green boundary shown in the figure 5.1-2 below. Any point outside this hexagon is considered to be in the failure region[3]. Maximum shear stress can be found using the equation 5.1-3 below[3].

$$\tau_{max} = \frac{\sigma_1 - \sigma_2}{2} \tag{5.1-3}$$

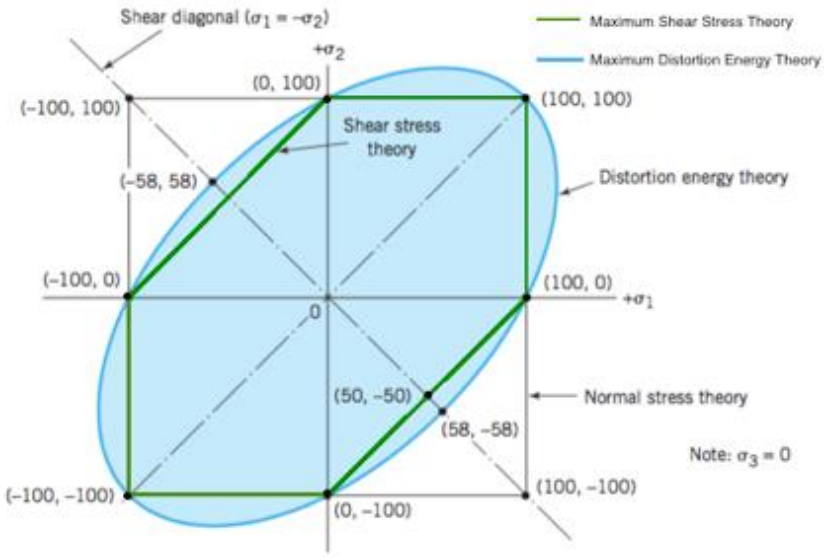

Figure 5.1-1: Maximum Shear Stress Theory and Maximum Distortion Energy Theory on a σ_1-σ_2 plot

Another popular theory is Mohr theory developed for brittle materials. This is a modification of maximum shear stress theory in which the failure envelope is constructed by connecting the opposite corners of quadrants I and III as shown in figure 5.1-2[2]. Any point outside the blue region will tend to fracture.

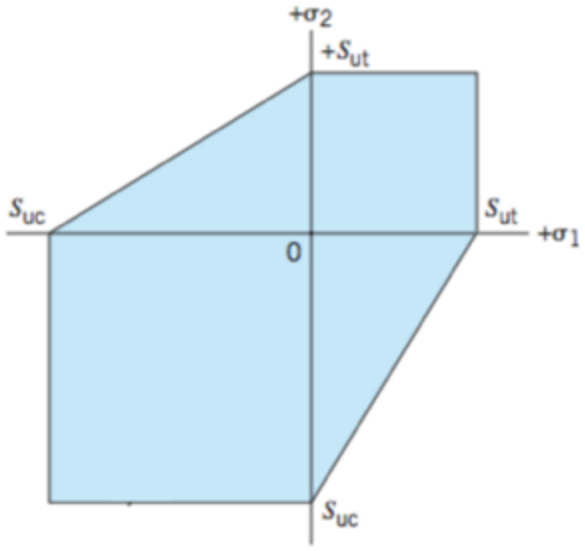

Figure 5.1-2: Graphical Representation of Mohr Theory

However, it was found that this a small modification was needed to fit to the real world applications. Therefore, figure 5.1-3 displays a more comprehensive way of Mohr theory by taking into account its application from experimental results. All these diagrams and theories are postulated such that they can fit the experimental data the best. We, as designers, have an immense responsibility to decide which theories to analyse our mechanical system with[4]. These theories are only for biaxial loadings, which is assuming that σ_3 is 0 and the principal stresses are on the axis.

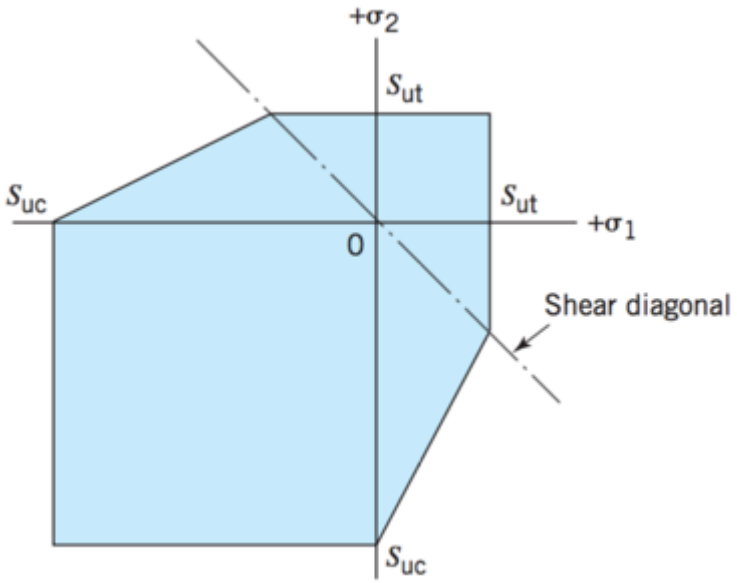

Figure 5.1-3: Graphical representation of Modified Mohr Theory

All the above diagrams have been drawn for biaxial loading. This is where the specimen is held in two dimensions and stress is applied on two sides, leaving one side blank. This alone is hard experiment to carry out, however, a triaxial loading can also take place, where stress is applied in all three directions and the strain is observed in each direction in relation to the normal and shear stress[5].

In relation to above all, some fracture mechanisms are for brittle materials and some for ductile, therefore, it is substantial to differentiate them. The fundamental differences between the two is that the ductile materials go through plastic deformation, however, brittle materials fracture before yielding. The table 5.1-1 below provides further details[6].

Table 5.1-1: Differences between ductile and brittle materials

Category	**Ductile**	**Brittle**
Deformation	Extensive	Little
Track propagation	Slow, needs stress	Fast
Type of Materials	Most metals (not too cold)	Ceramics, ice, cold metals
Warning	Permanent elongation	None
Strain (Distortion) energy	Higher	Lower
Fractures surface	Rough	Smoother
Necking	Yes	No

The strain energy is very important for fracture since this increases the effective strain in the maximum Distortion energy failure theory equation.

5.2 Fatigue Tests

The above mentioned failure mechanisms are for just one time loading and its effect on the failure. However, in real circumstances, the stress never exceeds the yield stress but still the mechanical components break. This is due to enormous cycles that take place going from compression to tension back to back. This is why there are various tests to carry out these experiments so that the specimen go under such stresses.

One of these tests is called the rotating bending. The figure 5.2-1 below gives a free body diagram of the experimental set up[7]. A weight w is applied on the specimen, which converts to w/2 on each side

of the specimen. This causes a bending stress. The motor moves the weight to point up and down alternatively, sometimes even at the rates of 1750rpm[2]. When the weight falls, the cycle counter stops and the total number of cycles are recorded. To experiment with different bending stresses, different weights are used.

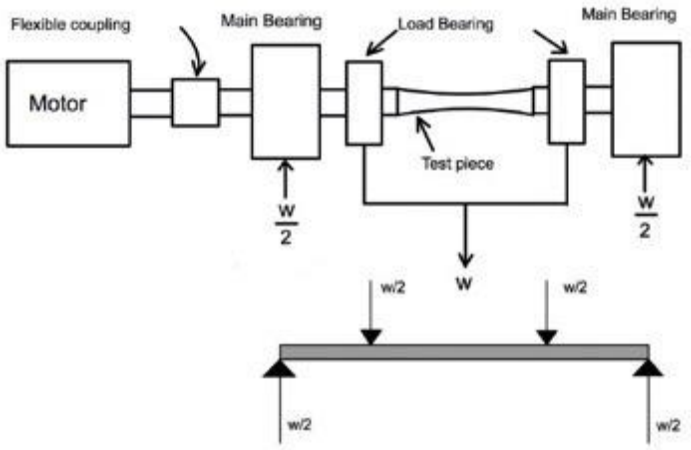

Figure 4.2-1: Rotating Bending test for bending stress

A sample test result is shown below in the figure 5.2-1[2].

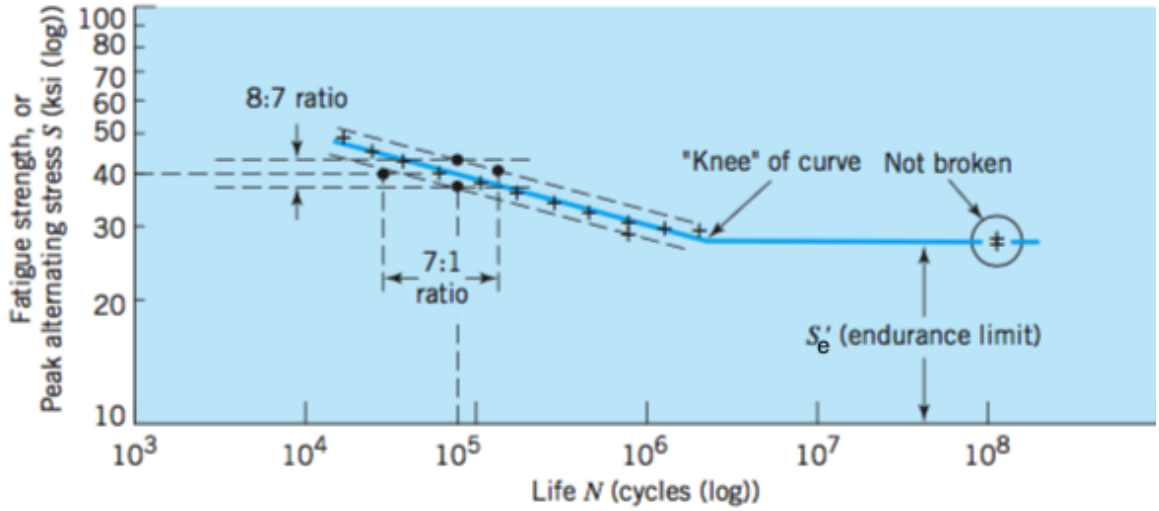

Figure 5.2-2: S-N plots of representative fatigue data for 120 BhN Steel

The graph above is called the S-N graph, where S or Fatigue Strength is on the y-axis and Number of cycles (N) the specimen goes under is on the x axis on a logarithmic scale[2]. The figure 5.2-2 is for 120BhN steel. We observe that as the number of cycles increase, the capacity for fatigue strength decreases until the material reaches its "knee" at the endurance limit. After this knee position, the fatigue strength stays the same for all the cycles and the specimen is supposed to have an infinite life at this fatigue strength.

Another kind of testing procedure is called reversed bending. This is very similar to rotating bending but instead of the motor applying a bending stress on both the sides of the specimen, the motor only applies the stress on one side and the other end remains stationary. The figure 5.2-3 below displays this test.[8] The machine applied a weight w on the right side of the specimen and creates a bending stress at the entire cross-section.

Figure 5.2-3: Reverse Bending

In reverse bending the fracture will most certainly arise from either the top or the bottom of the specimen and never from the middle. This is because the top and bottom are regions of the maximum bending stress. However, this is different in the rotating bending test. The failure here would happen from the surface at the top as the surface at the top and in the middle experiences the maximum bending stress.

Similar to this is also reversed axial loading, where a vertical load is applied to the side of the specimen where the other side remains fixed. This is shown in figure 5.2-4.[8] it is found that the reversed axial bending stress give 10% lower endurance limit in comparison to rotating bending. Reversed Axial loading subjects the entire cross section to the maximum stress, which is why the stress is more distributed and it fractures faster.

Figure 5.2-4: Reversed Axial Bending

Finally, another test is called the reversed torsional bending. In this experiment, a torque is provided on the right side of the specimen. This is an extremely important test for ductile materials and takes into account the distortion energy shown in figure 5.2-5[8].

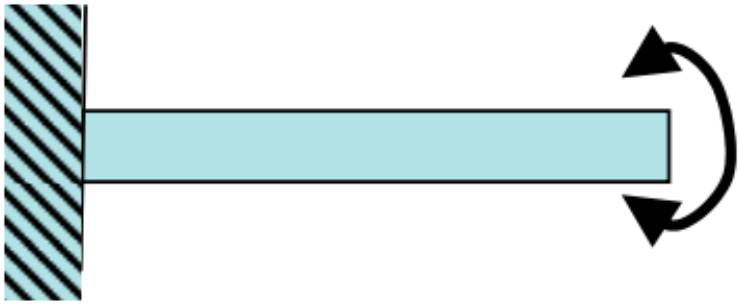

Figure 5.2-5: Reversed Torsional Loading

Finally, the reversed biaxial loading is when stress is applied onto a specimen from two different directions. This is shown in figure 5.2-6.

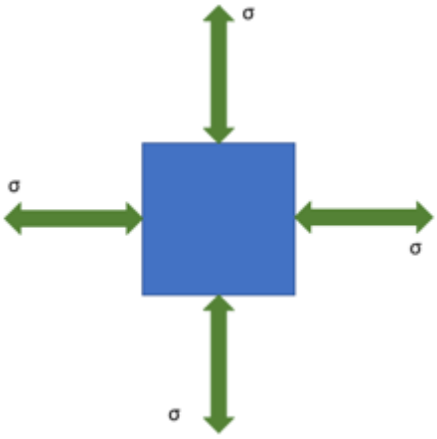

Figure 5.2-5: Reverse Biaxial Loading

As discussed in the chapter 3 and 4, there is a force and moment that acts only on one side of the lug stud. The other side of the stud remains stationary and touches the rim. This is why the reversed axial and reverse bending loading tests are the best for the scenario of the lug stud. These are the tests we need to analyse to create a S-N plot for the wheel lug stud of Toyota RAV4 XLE 2015.

5.3 Fatigue Factors

In order to carry out a fatigue test, we have numerous factors we need to start using the models. This section highlights these factors.

Stress endurance limit (S_e'), as pointed out in figure 5.2-2, is defined as "the maximum completely reversing cyclic stress that a material can withstand for indefinite (or infinite) number of stress reversals."[9] This is the maximum alternating strength at which the mechanical component has an infinite life. However, the actual endurance stress is experimentally found to be slightly less than this actual value found. This is why S_e' is multiplied by a factor to adjust to this factor (S_e). Because of this, the actual endurance limit is slightly lower than that found through theory. This is a slightly more conservative approach towards the endurance limit.

In these journal papers found (*Effect of surface finish on Fatigue Strength* by Mohamed Bayoumi[10] and *Effects of microstructure and surface roughness on the fatigue strength of high-strength steels* by Junbio Lai[11]) , the authors suggest a heavy dependence of endurance limit on surface roughness. They have proposed various models to assign these. If there is a surface roughness, it already creates the surface cracks that lead to fatigue mechanisms and failure can happen easily while testing. Therefore, the smoother the surface, the higher the endurance limit is predicted to be.

$$S_e = C_L C_G C_S C_T C_R S_e' \quad (5.3\text{-}1)$$

Where C_L is the load factor, C_G is the gradient factor, C_S is the surface factor, C_T is the temperature factor and C_R is the reliability factor. All of these factors vary from material to material. The table below provides the value along with the description of why they were chosen.

Table 5.3-1: Factors for Endurance Factor

	Description	Axial	Bending	Why
C_L	Load factor	1.0	1.0	
C_G	Gradient factor	1.0	0.7	Interpolation. The diameter 12mm, close to 10mm.
C_S	Surface Factor	0.34	0.34	Forged material from figure 8.13[2]
C_T	Temperature factor	1.0	1.0	Temperature is less than 840°F
C_R	Reliability factor	0.814	1.0	Assuming 99% reliability of factors

$$S_e = 0.7 * 0.34 * 0.814 S_e' \quad (5.3\text{-}2)$$

$$S_e = 0.194 S_e' \quad (5.3\text{-}3)$$

Another factor we need to calculate before fatigue analysis is stress concentration factor. It is found that there is a ratio between a notched and unnotched endurance limit and this factor is known as the stress concentration factor (K_f).[2] This value is calculated to be 4.3.[12] We would like K_f to be equal to the theoretical geometric factor, however, it is often less than that. Therefore, various models have to be taken into account numerous other models. This happens because our lug stud is not completely symmetric and has various other internal irregularities, which causes it to have local stresses. Therefore, this factor can be calculate using equation 5.3-4.

$$K_f = 1 + (K_t - 1)q \quad (5.3\text{-}4)$$

Where q changes from material to material and is the notch sensitivity factor. It is 0.7 for steel.[12] Therefore, K_f is equal to 3.31.

The table below provides all the factors required for fatigue model analysis.

Table 5.3-2: Fatigue Analysis variables

Parameter	Description	**Value in English Units**	**Value in Metric units**
S_u	Ultimate Tensile Strength	151 ksi	1040 MPa
S_y	Ultimate Yield Strength	136ksi	940 MPa
$-S_y$	Compressive Yield Strength	N/A	N/A
S_e	Endurance Limit	75.5 ksi	520 MPa
K_f	Fatigue Concentration Factor	3.31	3.31
q	Notch Sensitivity Factor	0.7	0.7
C_L	Bending Load	0.277	0.277
	Axial Load	0.238	0.238
C_S	Surface Factor	0.34	0.34
C_G	Gradient factor	0.7	0.7
C_T	Temperature factor	1.0	1.0
C_R	Reliability factor	0.814	0.814
K_t	Concentration notch	4.3	4.3

5.4 Cook Fatigue Model

In order to find the cook plot we have to find some basic quantities. The formulaes are stated in equations below.

$$S_a = \frac{S_e}{K_f}\left(\frac{1 - \frac{S_y}{S_u}}{1 - \frac{S_e}{S_u}}\right) \quad (5.4\text{-}1)$$

$$S_{m1} = \frac{S_y}{K_t} - S_a \quad (5.4\text{-}2)$$

$$S_{m2} = S_y - S_a \quad (5.4\text{-}3)$$

$$\sigma_a = \frac{S_e}{K_f}\left(1 - \frac{K_f \sigma_m}{S_u}\right),\ 0 \le \sigma_m \le S_{m1} \quad (5.4\text{-}4)$$

$$\sigma_a = \frac{S_e}{K_f}\frac{\left(1 - \frac{S_y}{S_u}\right)}{\left(1 - \frac{S_e}{S_u}\right)},\ S_{m1} \le \sigma_m \le S_{m2} \quad (5.4\text{-}5)$$

$$\sigma_a = S_y - \sigma_m, S_{m2} \leq \sigma_m \leq S_y \quad (5.4\text{-}6)$$

Using all of these values, we can plot these curves on a σ_1-σ_2 plot like below.

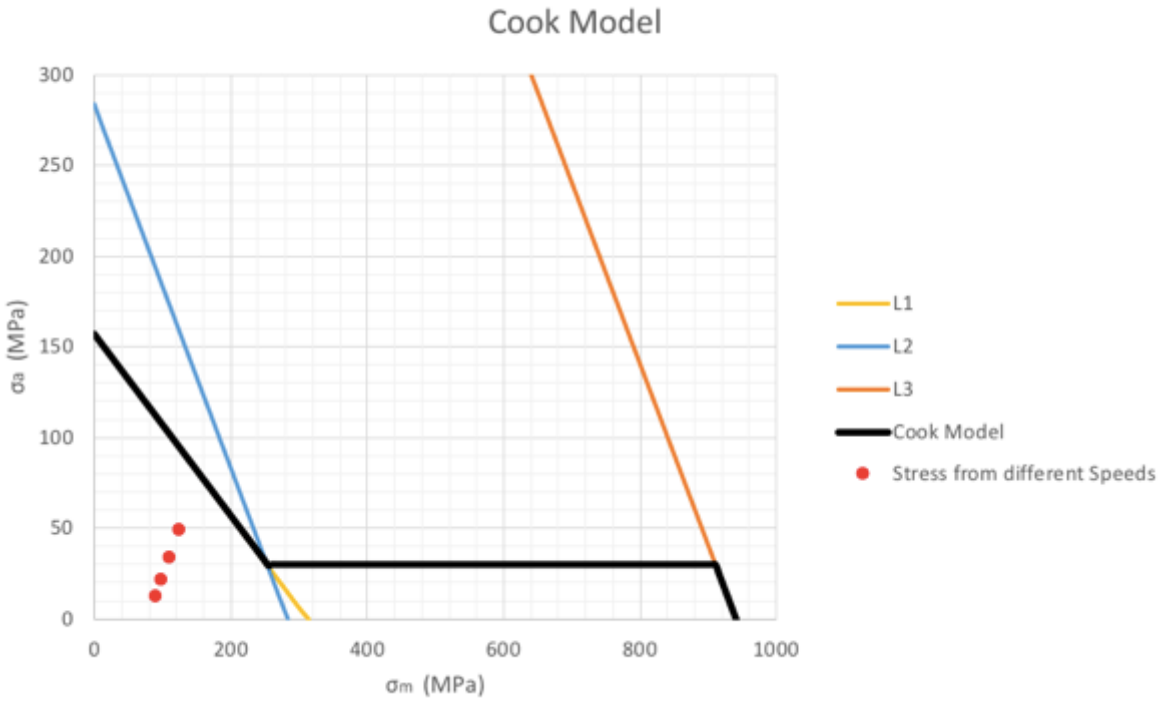

Figure 5.4-1: Cook model for a lug stud

It can be seen that all the red points we got from chapter 4 are under the curve, which means that at the applied stress, there is not failure likely to happen. All the parameters used to plot the above curve are provided in the table 5.4-1 below:

Table 5.4-1: Cook plot values

Parameters	Value
Kf/Su	0.00
Sy / Kf	283.99
Se / Kf	157.10
Su/Kf	314.20
Sy/Su	0.90
Se/Su	0.50
Sm1	253.78
Sm2	909.79
Sa	30.21

5.5 Gunn Fatigue Model

Another model used to calculate the model for fatigue analysis is Gunn Model. The parameters needed to calculate these are given below.

Our first goal is to find the S_a so that we can calculate all the other values based on that. This is complicated process.

$$X_N = \frac{\left[\frac{S_y}{S_e} - 1\right]}{\left[\frac{S_u}{S_e} - 1\right]} \tag{5.5-1}$$

$$X_{N+1} = \frac{\left[\frac{S_y}{S_e} - 1\right] + \left[X_N^{4/3} - X_N\right]}{\left[\frac{S_u}{S_e} - 1\right]} \tag{5.5-2}$$

The value of X_{N+1} converges really fast. These have been shown in the table 5.5-1 below.

Table 5.5-1: Table to find X_N

x0	0.80769231
x1	0.75219065
x2	0.73957695
x3	0.73693829
x4	0.73639721
x5	0.73628673
x6	0.73626419
x7	0.73625959
x8	0.73625865
x9	0.73625846
x10	0.73625842
x11	0.73625841
x12	0.73625841

The value of X converges to 0.736.

$$S_a = \frac{S_u}{K_t} X \tag{5.5-3}$$

$$\sigma_a = \frac{S_e}{K_t}\left(1 - \left(\frac{K_f \sigma_m}{S_u}\right)^{4/3}\right), 0 \le \sigma_m \le S_a \tag{5.4-3}$$

$$\sigma_a = \sigma_a^*, S_a \le \sigma_m \le S_y \tag{5.5-4}$$

Just using these equations, we can calculate the following parameters.

Table 5.5-2: Gunn Model Parameters

Parameters	**Value**
Sy/Se	1.80769231
Kt/Su	0.00413462
Sy / Kt	218.604651

Se / Kt	120.930233
Su/Kt	241.860465
Sy/Su	0.90384615
Se/Su	0.5
Sa	178.071802

Using all of these parameters, we can calculate the Gunn Plot in the figure 5.5-1.

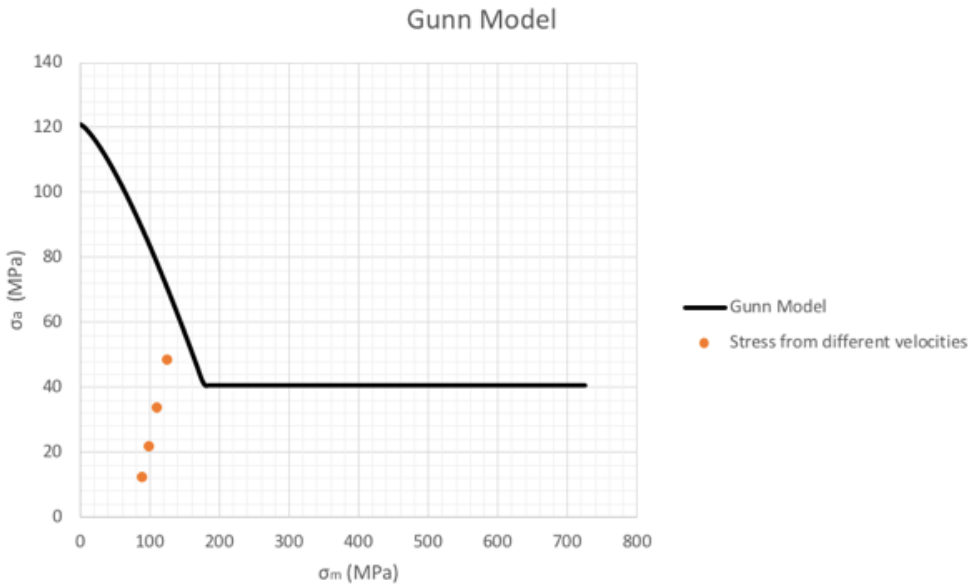

Figure 5.5-1: Gunn Model Plot

As it can be seen from the graph, all the velocities lie under the graph. This means that none of the velocities we are concerned with would affect the failure fatigue.

5.6 Fatigue Safety Factor and Most Relevant Fatigue Model

Safety factor is an important value to calculate and should not be neglected. Due to an improper analysis, it was not included in this study.

In the case we are looking at, both the models seem to work. As we only tested for 15, 20, 25 and 30 mph speed, the values for the alternating stress seem to be under the curve in both the circumstances. However, cars obviously go above the speed of 30 mph on a daily basis. In both the graphs, it seems that if we interpolate the values, they will very soon go above the graph. This suggests that both the models are very conservative. The Toyota RAV4 XLE 2015 can obviously go above the speed of at least 80mph and therefore, both the graphs underestimate the fatigue failure analysis. However, to compare the both, the Cook model seems to be more conservative in comparison to Gunn model after Sm1 value is reached.

5.7 Table of Data

Table 5.1-1: Differences between ductile and brittle materials

Category	**Ductile**	**Brittle**
Deformation	Extensive	Little
Track propagation	Slow, needs stress	Fast
Type of Materials	Most metals (not too cold)	Ceramics, ice, cold metals
Warning	Permanent elongation	None

Strain (Distortion) energy	Higher	Lower
Fractures surface	Rough	Smoother
Necking	Yes	No

Table 5.3-2: Factors for Endurance Factor

	Description	Axial	Bending	Why
C_L	Load factor	1.0	1.0	
C_G	Gradient factor	1.0	0.7	Interpolation. The diameter 12mm, close to 10mm.
C_S	Surface Factor	0.34	0.34	Forged material from figure 8.13[2]
C_T	Temperature factor	1.0	1.0	Temperature is less than 840°F
C_R	Reliability factor	0.814	1.0	Assuming 99% reliability of factors

Table 5.3-2: Fatigue Analysis variables

Parameter	Description	**Value in English Units**	**Value in Metric units**
S_u	Ultimate Tensile Strength	151 ksi	1040 MPa
S_y	Ultimate Yield Strength	136ksi	940 MPa
$-S_y$	Compressive Yield Strength	N/A	N/A
S_e	Endurance Limit	75.5 ksi	520 MPa
K_f	Fatigue Concentration Factor	3.31	3.31
q	Notch Sensitivity Factor	0.7	0.7
C_L	Bending Load	0.277	0.277
	Axial Load	0.238	0.238
C_S	Surface Factor	0.34	0.34
C_G	Gradient factor	0.7	0.7
C_T	Temperature factor	1.0	1.0
C_R	Reliability factor	0.814	0.814
K_t	Concentration notch	4.3	4.3

Table 5.4-1: Cook plot values

Parameters	**Value**
Kf/Su	0.00
Sy / Kf	283.99
Se / Kf	157.10
Su/Kf	314.20
Sy/Su	0.90
Se/Su	0.50
Sm1	253.78
Sm2	909.79
Sa	30.21

Table 5.5-1: Table to find X_N

x0	0.80769231

x1	0.75219065
x2	0.73957695
x3	0.73693829
x4	0.73639721
x5	0.73628673
x6	0.73626419
x7	0.73625959
x8	0.73625865
x9	0.73625846
x10	0.73625842
x11	0.73625841
x12	0.73625841

Table 5.5-2: Gunn Model Parameters

Parameters	**Value**
Sy/Se	1.80769231
Kt/Su	0.00413462
Sy / Kt	218.604651
Se / Kt	120.930233
Su/Kt	241.860465
Sy/Su	0.90384615
Se/Su	0.5
Sa	178.071802

5.8 References

[1] "Fatigue (Material)." Wikipedia, Wikimedia Foundation, 18 Feb. 2018, en.wikipedia.org/wiki/Fatigue_(material).
[2] Juvinall, Robert C., and Kurt M. Marshek. Fundamentals of Machine Component Design. John Wiley & Sons, 2017.
[3] "Theories of Elastic Failure - Lecture 35." NPTEL, nptel.ac.in/courses/112107146/lects%20&%20picts/image/lect35/lecture35.htm.
[4] Agarwa;, Abhishek, director. Dr. Abdul Kalam. Dr. Abdul Kalam, Dream Merchants Inc.
[5] "Triaxial Compression Tests." RISE - Research Institutes of Sweden, www.sp.se/en/index/services/rockmechanicaltesting/triaxial/sidor/default.aspx.
[6] "Failure." Virginia.edu - MSE 209 Chapter 8, www.virginia.edu/bohr/mse209/chapter8.htm
[7] Kim, Sangone. "Smart Testing." Fatigue Test, kstestmc.blogspot.com/p/fatigue-test.html.
[8] "Fatigue." Mississippi State University - Mechanical Engineering.
[9] "Design for Cyclic Loading." New Jersey Institute of Technology, web.njit.edu/~sengupta/met%20301/cyclic_loading%20indefinite.pdf.
[10] Effect of surface finish on Fatigue Strength

[11] Lai, Junbiao, et al. “Effects of Microstructure and Surface Roughness on the Fatigue Strength of High-Strength Steels.” Procedia Structural Integrity, vol. 2, 2016, pp. 1213–1220., doi:10.1016/j.prostr.2016.06.155.
[12] Burguete, R L, and E A Patterson. “The Effect of Mean Stress on the Fatigue Limit of High Tensile Bolts Burguete, R.L. and Patterson, E.A. Proc. Inst. Mech. Eng B, J. Engng Manufacture (1995) 209 (C4), 257â“262 ISSN: 0954-4054.” International Journal of Fatigue, vol. 19, no. 5, 1997, p. 441., doi:10.1016/s0142-1123(97)90094-3.

5.9 Level of effort

I spent about 25 hours on this project.